

Original Research

Bioinformatic Analysis and Experimental Validation of Ubiquitin-Proteasomal System-Related Hub Genes as Novel Biomarkers for Alzheimer's Disease

Yuting Zhang^{1,†}, Jie Wu^{2,†}, Guoxing You¹, Wenjie Guo¹, Yupeng Wang^{1,3}, Zhiyong Yu¹, Yan Geng¹, Qinghua Zhong¹, Jie Zan^{1,*}, Linbo Zheng^{3,*}¹School of Biomedical and Pharmaceutical Sciences, Guangdong University of Technology, 510006 Guangzhou, Guangdong, China²The Second School of Clinical Medicine, Southern Medical University, 510515 Guangzhou, Guangdong, China³Department of Traditional Chinese Medicine, Guangdong Second Provincial General Hospital, 510310 Guangzhou, Guangdong, China*Correspondence: zanj@gdut.edu.cn (Jie Zan); zhenglinbo1987@163.com (Linbo Zheng)

†These authors contributed equally.

Academic Editor: Hongmin Wang

Submitted: 14 May 2023 Revised: 11 June 2023 Accepted: 19 June 2023 Published: 18 October 2023

Abstract

Background: Alzheimer's disease (AD) is a common progressive neurodegenerative disease. The Ubiquitin-Protease system (UPS), which plays important roles in maintaining protein homeostasis in eukaryotic cells, is involved in the development of AD. This study sought to identify differential UPS-related genes (UPGs) in AD patients by using bioinformatic methods, reveal potential biomarkers for early detection of AD, and investigate the association between the identified biomarkers and immune cell infiltration in AD. **Methods:** The differentially expressed UPGs were screened with bioinformatics analyses using the Gene Expression Omnibus (GEO) database. A weighted gene co-expression network analysis (WGCNA) analysis was performed to explore the key gene modules associated with AD. A Single-sample Gene Set Enrichment Analysis (ssGSEA) analysis was performed to explore the patterns of immune cells in the brain tissue of AD patients. Real-time quantitative PCR (RT-qPCR) was performed to examine the expression of hub genes in blood samples from healthy controls and AD patients. **Results:** In this study, we identified four UPGs (*USP3*, *HECW2*, *PSMB7*, and *UBE2V1*) using multiple bioinformatic analyses. Furthermore, three UPGs (*USP3*, *HECW2*, *PSMB7*) that are strongly correlated with the clinical features of AD were used to construct risk score prediction markers to diagnose and predict the severity of AD. Subsequently, we analyzed the patterns of immune cells in the brain tissue of AD patients and the associations between immune cells and the three key UPGs. Finally, the risk score model was verified in several datasets of AD and showed good accuracy. **Conclusions:** Three key UPGs are identified as potential biomarker for AD patients. These genes may provide new targets for the early identification of AD patients.

Keywords: AD; machine learning; Ubiquitin-Protease; biomarkers; bioinformatic

1. Introduction

Alzheimer's disease (AD) is a progressive neurodegenerative disease characterized by memory deficits and cognitive impairments. Approximately 55 million people worldwide were diagnosed with AD in 2021. Most AD cases occur after the age of 65 and the average living period of AD patients over 65 is 4 to 8 years. From the pathological point of view, AD is characterized by amyloid-beta ($A\beta$) accumulation and tau aggregates [1,2]. Numerous studies suggest that $A\beta$ accumulation in the brain starts more than ten years prior to the onset of AD symptoms [3–5]. Thus, clearing $A\beta$ deposits is a promising therapeutic strategy to mitigate AD [6–8].

The Ubiquitin-Protease system (UPS), which degrades dysfunctional/misfolded proteins, plays an important role in maintaining protein homeostasis in eukaryotic cells [9]. The UPS is also involved in several physiological processes, such as cell survival, differentiation, and innate immunity [10–12]. Dysfunction of the UPS triggers var-

ious diseases including tumors, cardiac pathophysiology, Parkinson's disease, and AD [13–16]. A previous study reported that UPS dysfunction promoted $A\beta$ accumulation via increasing α -secretase in neurons of AD [17]. Additionally, proteasomal activity in the AD brain is evidently decreased [18] and UPS dysfunction leads to synaptic plasticity impairments in AD [19,20]. Thus, clarifying the molecular mechanism underlying UPS dysfunction in AD is essential for finding new diagnostic markers for AD and developing potential therapeutic drugs.

With the ability to quickly and accurately analyze large data sets, bioinformatics has been extensively used to analyze disease characteristics and identify early diagnostic markers of diseases [21,22]. For example, through bioinformatic analysis, a prognostic risk model for head and neck squamous cell carcinoma based on eight UPS-related genes (UPGs) was established [23]. A high-risk group of lung adenocarcinoma patients showed higher mutation and tumor mutation burden, analyzed by bioinformatics [24]. However, no study has focused on which UPGs are critical



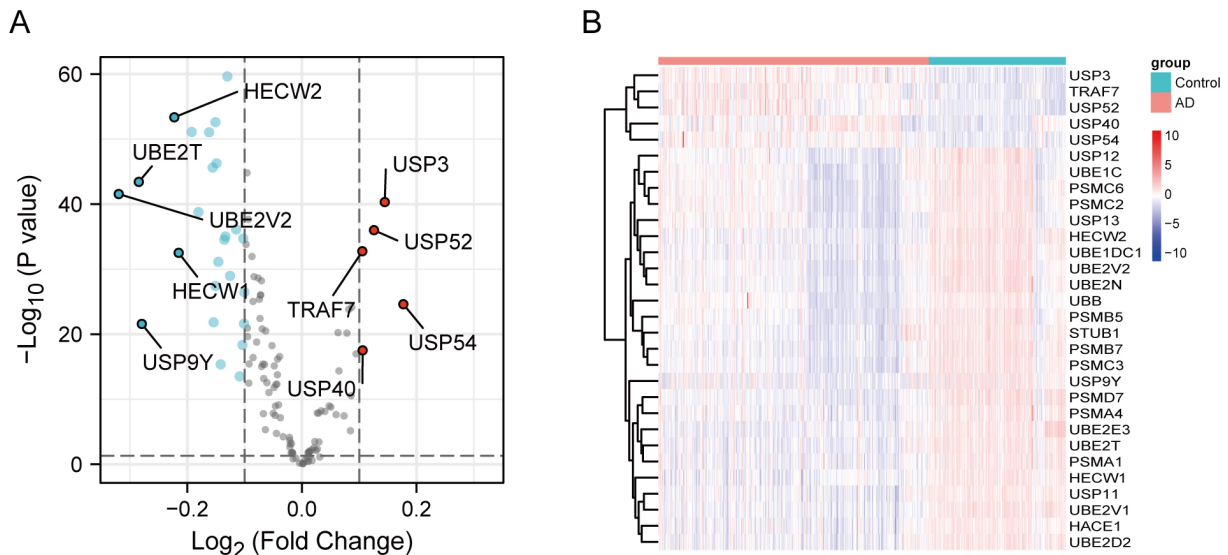


Fig. 1. Identification of UPDEGs in AD. (A) Differentially expressed UPG between AD patients and healthy controls in GSE33000. The screening criteria were $|\text{LogFC}| > 0.1$ and p value < 0.05 . (B) Heatmap of the differential UPGs in GSE33000. UPDEGs, UPS-related differentially expressed genes; AD, Alzheimer's disease; UPG, UPS-related gene; UPS, Ubiquitin-Proteasome system.

for AD development. In addition, immune cell infiltration has been found in the brains of clinical AD patients [25] and depletion of natural killer (NK) cells relieved cognitive impairment in 3xTg-AD mice [26]. However, the relationship between UPGs and immune cell infiltration in AD patients' brains is not clear.

In the present study, we explore the differential UPGs in AD patients using bioinformatic methods, identify potential biomarkers for early detection of AD, and analyze the correlation between potential biomarkers and immune cell infiltration in AD.

2. Materials and Methods

2.1 Analysis of Differentially Expressed Genes

Data was downloaded from the Gene Expression Omnibus (GEO) database (<http://www.ncbi.nlm.nih.gov/geo>). According to AD patients' ID, patients' clinical data was screened using the following criteria: ① AD was diagnosed via NINCDS-ADRDA and DSM-IV criteria, ② available expression profile, and ③ available year data. GSE33000 included the mRNA expression profiles of brain tissue from 310 AD patients and 157 healthy controls. GSE5281, GSE26972, GSE29378, GSE36980, GSE48350, and GSE63060 were used as validation sets. GSE5281 included the transcriptional profiles of 74 AD brain samples and 87 healthy control samples. GSE26972 included the transcriptional profiles of 3 AD brain samples and 3 healthy control samples. GSE29378 included the transcriptional profiles of 31 AD brain samples and 32 healthy control samples. GSE36980 included the transcriptional profiles of 33 AD brain samples and 47 healthy control samples. GSE48350 included the transcriptional profiles of

80 AD brain samples and 173 healthy control samples. GSE63060 included the blood RNA profiles of 49 AD samples and 64 healthy control samples. All of the above data was obtained from the Gene Expression Omnibus (GEO) (<https://www.ncbi.nlm.nih.gov/gds>). We downloaded the genes of the Ubiquitin-Proteasome pathway from the PathCards (<https://pathcards.genecards.org/>) by using keywords "Ubiquitin". Raw data from GEO data sets were annotated in line with their respective platform files and probes were converted to gene symbols. The software Perl and R (version 4.0.2) (<https://www.r-project.org/>) were used for data preprocessing. The "limma" [27] R-package was utilized to determine the differentially expressed genes (DEGs) from GSE33000 using $|\log\text{FC}| > 0.1$ and $\text{Adj. } p \text{ Val} < 0.05$. Venn diagrams were used to analyze the UPS-related differentially expressed genes (UPDEGs). Volcano plots and heatmaps were used for visualization.

2.2 Weighted Gene Co-Expression Network Analysis (WGCNA)

The "Weighted Gene Co-Expression Network Analysis (WGCNA)" [28] R-package was utilized to analyze module identification. A topological overlap matrix [29] was performed to analyze the connection strength between genes (Dynamic Tree Cut: $\text{minModuleSize} = 50$; Cluster Cut: $\text{MEDissThres} = 0.25$). Candidate modules were defined as significantly correlated with AD.

2.3 Functional Enrichment Analysis

The "clusterProfiler" R-package was utilized to analyze the biologic processes (BP), cellular components (CC), and molecular functions (MF) enrichment analysis of DEGs. The potential enriched signals were analyzed via

Kyoto Encyclopedia of Genes and Genomes (KEGG) (<http://www.kegg.jp/>). False Discovery Rate (FDR) <0.05 was considered significant.

2.4 Construction and Validation of Predictive Model

Least absolute shrinkage and selection operator (LASSO) regression, random forest, and Support Vector Machine-Recursive Feature Elimination (SVM-RFE) [30] were used to establish the diagnostic model using the most representative genes. The “glmnet”, “random Forest”, “caret” packages were applied for this study. A Venn diagram was used to visualize the intersection of the above three methods. The screened genes were used for construction of the diagnostic model. Riskscores were obtained using the following formula: $\text{riskscore} = \sum (\beta_i \times \text{Exp}_i)$, where β_i represented the corresponding regression coefficients of each candidate prognostic gene and Exp_i was the candidate gene's expression value. The “pROC” R-package was utilized to analyze the receiver operating curve (ROC) curve.

2.5 Correlation of Clinical Characteristics and UPG

GSE106241 was used to study the correlation between clinical features and UPGs in AD patients. GSE106241 included the gene expression profiles of 60 AD brain samples with different clinical traits (Braak stages, alpha-, beta-, gamma-secretase activity, and amyloid-beta 42 levels). The R-packages “ggplot2” and “ggpubr” were used to visualize the correlation between clinical features and UPG on a violin plot.

2.6 Consensus Clustering

Key UPGs were selected to analyze the different subpopulations in AD by using “ConsensusClusterPlus” [31] packages. The cumulative distribution function (CDF) and total CDF curve area (delta area) were used to select the optimal cluster number. A Gene Set Variation Analysis (GSVA) analysis was performed using the “h.all.v7.5.1. symbols” files downloaded from the MSigDB online database (<https://www.gsea-msigdb.org/gsea/msigdb/index.jsp>). “GSVA” packages was used to analyze the different pathways among the three clusters. The expression of 28 immune cell types in each sample were analyzed using single-sample Gene Set Enrichment Analysis (ssGSEA).

2.7 Sample Collection

The study protocol was approved by the Ethics Committee of the Guangdong Second Provincial Hospital (20191121-01-YXKXYJ-SZRLH2020) and adhered to the tenets of the Declaration of Helsinki. 10 blood samples were collected from 5 healthy controls and 5 patients with AD.

2.8 Real-Time Quantitative PCR (RT-qPCR)

Total RNA was isolated using an RNA extraction kit (12183020, Thermo Fisher Scientific, Waltham, MA,

USA) and reverse-transcribed into cDNA using Prime-Script RT Master Mix (RR036A, Takara, Tokyo, Japan). Subsequently, cDNAs were used for real-time quantitative PCR (RT-qPCR) analysis with the ABI StepOnePlus Real-Time PCR machine (ABI7500, Applied Biosystems, Foster City, CA, USA). The primer sequences were as follows: *USP3*, forward 5'- CAAGCTGGGACTGGTACAGAA -3' and reverse 5'- GCAGTGGTGCTTCCATTACTT -3'; *HECW2*, forward 5'- GCTTAGTGCCTGGCTTCTATGAGG -3' and reverse 5'- TGTGCCTGCATGACCAATTCC -3'; *PSMB7*, forward 5'- TTTCTCCGCCATACACAGTG -3' and reverse 5'- AGCACCTCAATCTCCAGAGGA -3'; *GAPDH*, forward 5'- GTCTCTCTGACTTCAACAGCG -3' and reverse 5'- AATGCTTGGGCTTGCATCA -3'. Statistically significant differences between groups were determined using unpaired *t* tests.

2.9 Statistical Analysis

Spearman's correlation coefficient was performed for correlation analyses. The Kruskal-Wallis test was used to analyze the continuous variables between the three groups. The Wilcoxon test was performed to analyze the continuous variables between the two groups. A *p* < 0.05 was regarded as statistically significant.

3. Results

3.1 Identification of UPDEGs in AD

Through the analysis of differentially expressed mRNA profiles from 310 AD patients and 107 healthy controls obtained from the GSE33000 dataset, 1593 significantly upregulated and 1974 significantly downregulated mRNAs were identified. Furthermore, by intersecting UPG and DEG, 5 significantly upregulated and 25 significantly downregulated UPDEGs were identified, as shown in Fig. 1A,B.

3.2 Identification of Key Modules through WGCNA

As shown in the **Supplementary Fig. 1A**, the soft threshold power value was set at 9 for scale-free network construction. A dendrogram was conducted to analyze module similarity via WGCNA (**Supplementary Fig. 1B**). The blue module showed a high connection with AD ($r = -0.62$, $p = 2 \times 10^{-50}$) (**Supplementary Fig. 1C**). The correlation of combined gene significance and the blue module membership is shown in **Supplementary Fig. 1D**. Therefore, the genes in the blue module were selected for subsequent analysis.

3.3 Enrichment Analysis of the Intersected Genes

Subsequently, 2410 genes were obtained through the intersection of the blue module and DEGs (Fig. 2A), and were further used for enrichment analysis. The BP analysis showed that signal transduction and nervous system development were enriched (Fig. 2B). The CC analysis showed

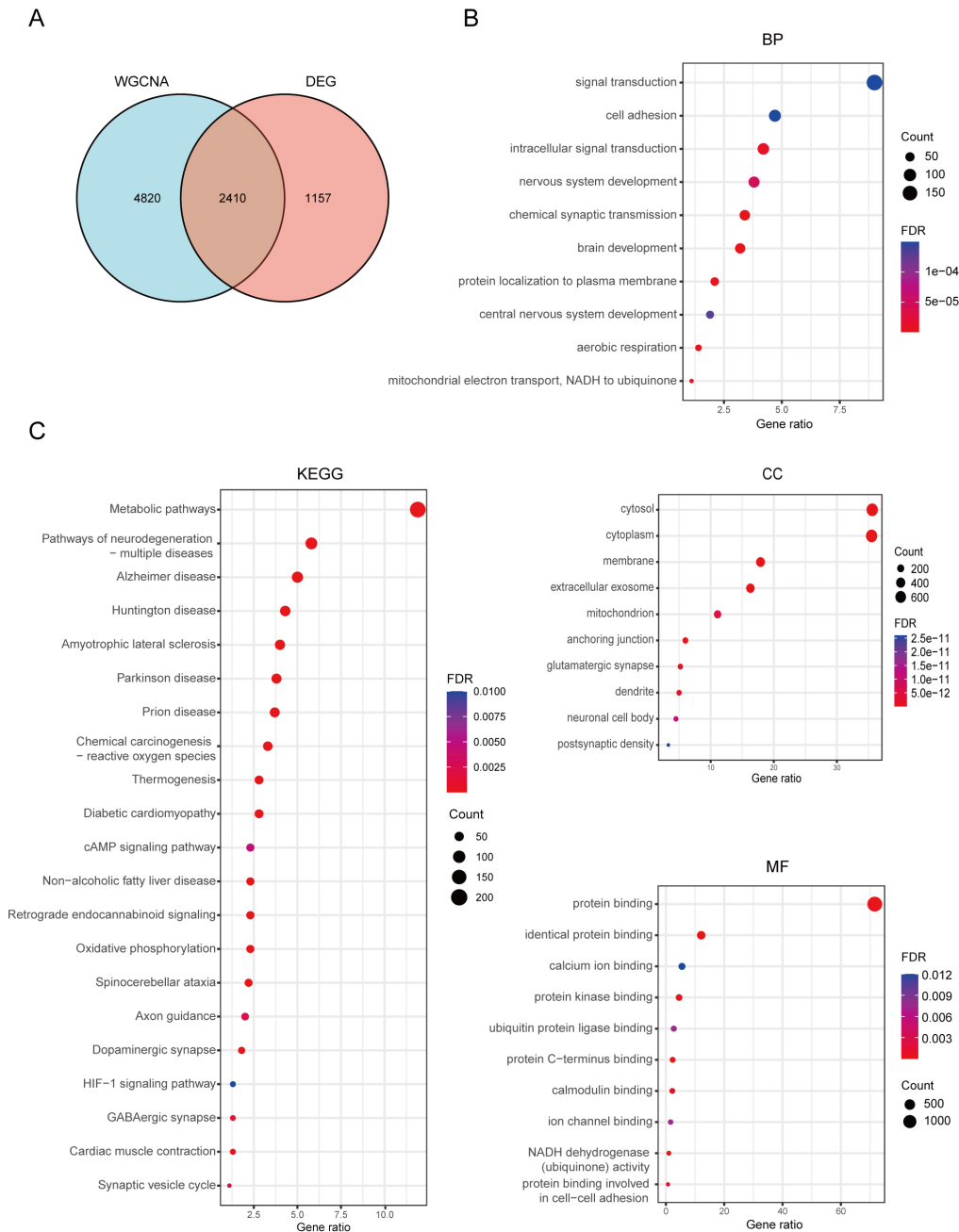


Fig. 2. Analysis of enrichment. (A) Overlapping genes of the blue module and DEGs. (B) GO analyses of intersection genes. (C) KEGG analysis of intersection genes. WGCNA, weighted gene co-expression network analysis; DEGs, differentially expressed genes; BP, biologic processes; GO, Gene Ontology; KEGG, Kyoto Encyclopedia of Genes and Genomes; CC, cellular components; MF, molecular functions; FDR, False Discovery Rate.

that the genes were mainly related to the cytosol, cytoplasm, membrane, and extracellular exosome (Fig. 2B). The MF results showed that protein binding and calcium ion binding were enriched (Fig. 2B). The KEGG enrichment analysis revealed that the genes were predominantly enriched in metabolic, neurodegeneration-multiple diseases, cyclic adenosine monophosphate (cAMP) signaling, and oxidative phosphorylation (Fig. 2C).

3.4 Identification of the UPS-Signature

There were 27 UPGs obtained through the intersection of the blue module and the differentially expressed UPGs (Fig. 3A). Furthermore, to identify the potential diagnostic biomarkers, we used the LASSO regression method (Fig. 3B), Support Vector Machine (SVM) (Fig. 3C,D), and random forest analyses (Fig. 3E). A 4-gene UPG-signature, including *USP3*, *HECW2*, *PSMB7*, and *UBE2V1*, was identified (Fig. 3F).

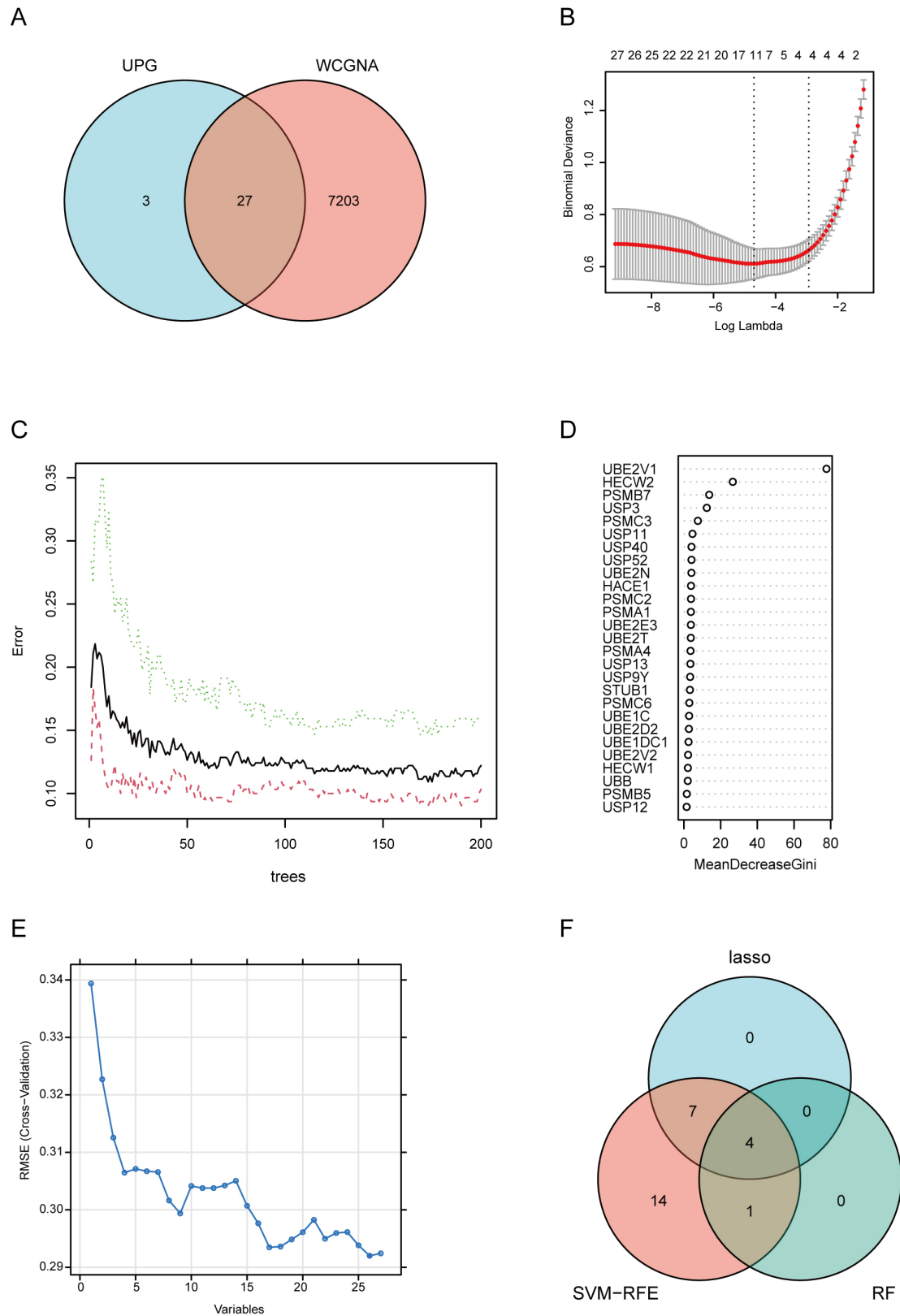


Fig. 3. Identification of key UPG. (A) Overlapping genes of the blue module and UPGs. (B–E) Screening the potential biomarkers via LASSO regression, SVM, and RF algorithm. (F) Venn diagram demonstrating the intersection of key UPGs obtained by three machine learning. LASSO, Least absolute shrinkage and selection operator; SVM, Support Vector Machine; SVM-RFE, Support Vector Machine-Recursive Feature Elimination; RF, Random forest.

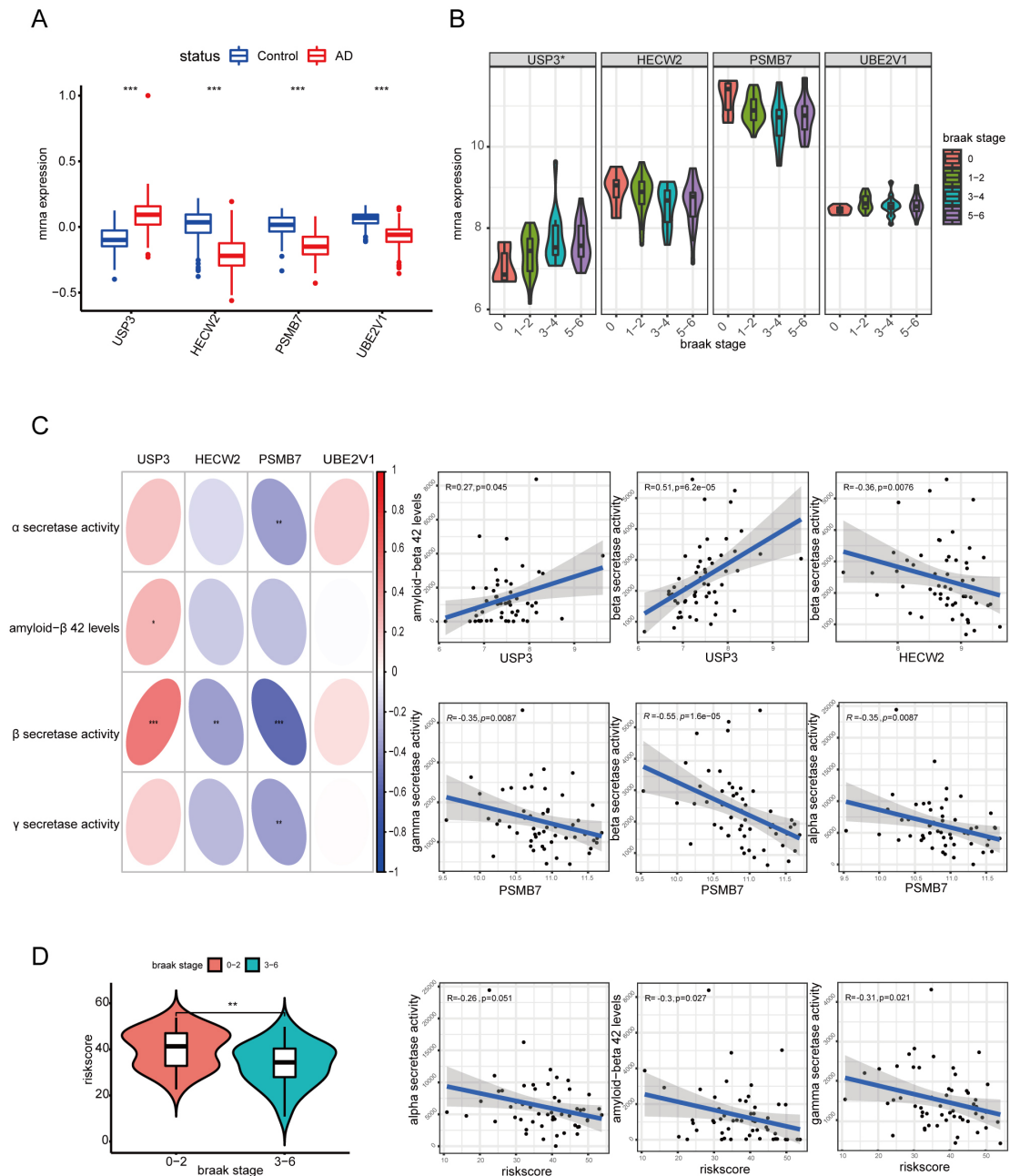


Fig. 4. Correlation between UPG and clinical Characteristics. (A) Differential expression of four UPG between AD and control. (B) Differential expression of four UPG in different Braak stages. (C,D) Correlation between four UPG, riskscore and clinical characteristics. * represents $p < 0.05$; ** represents $p < 0.01$; *** represents $p < 0.001$.

3.5 Correlation of Clinical Characteristics and UPG and Construction of Predictive Model

3.5.1 Relationships of the UPS-Signature Genes and Clinical Characteristics

Next, we explored expression of the UPS-signature genes and found that only *USP3* was highly expressed in the AD group. The expression of *HECW2*, *PSMB7*, and *UBE2V1* were all decreased in the AD group compared to the control group (Fig. 4A). Furthermore, we investigated the relationship between the UPS-signature genes and clinical characteristics in GSE106241 and found that *USP3* was

significantly associated with the Braak stages (Fig. 4B). While there were no significant differences among different Braak stages, the expression of *HECW2* and *PSMB7* were decreased in the high Braak stages (Fig. 4B). *UBE2V1* expression showed no evident change in different Braak stages (Fig. 4B). With regards to clinical manifestations, *USP3* was strongly correlated with amyloid-beta 42 levels and beta secretase activity, *HECW2* was negatively correlated with beta secretase activity, and *PSMB7* was negatively correlated with alpha secretase activity, gamma secretase activity, and beta secretase activity (Fig. 4C). Given

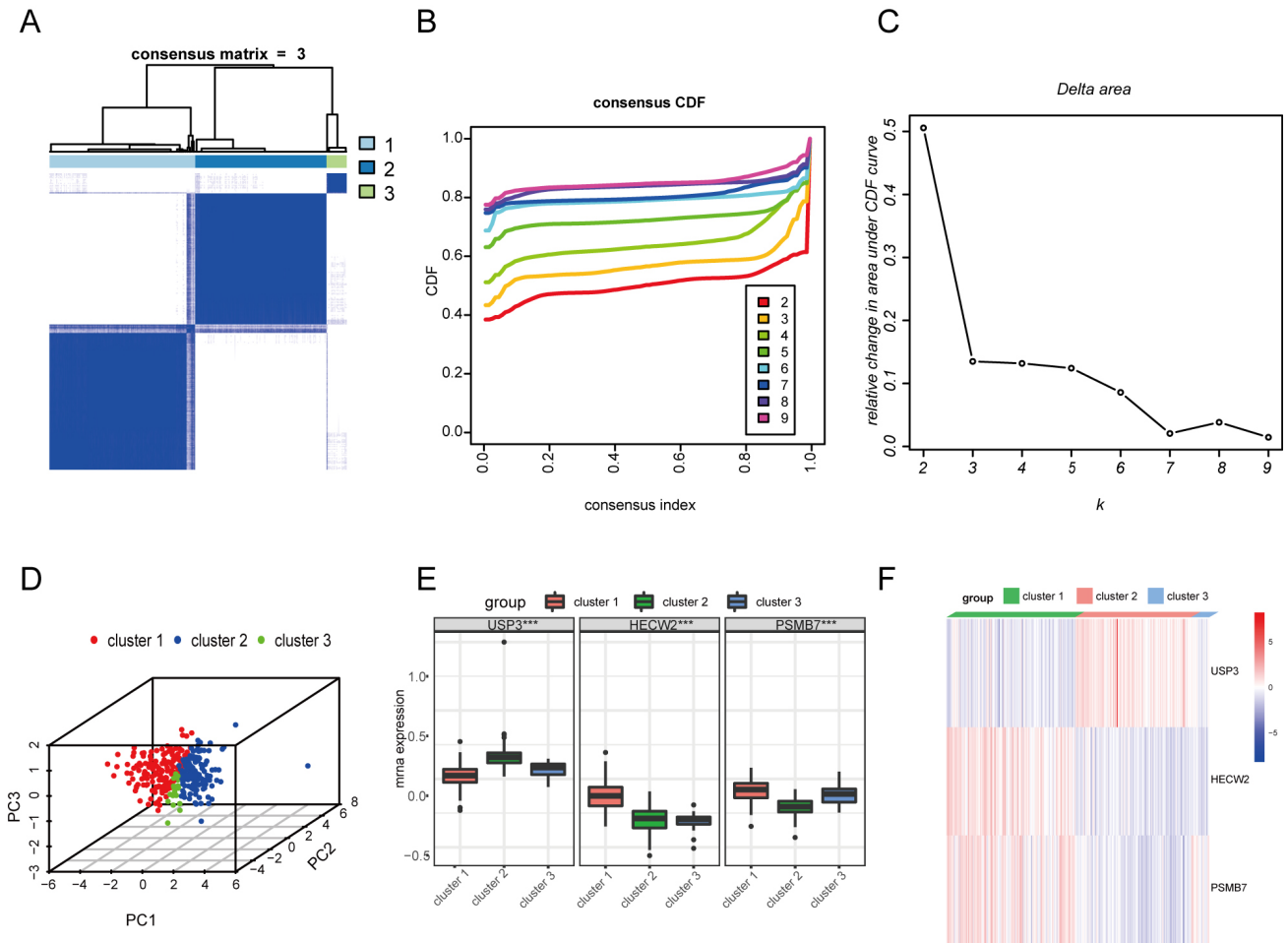


Fig. 6. Identification of ubiquitin-proteasomal subtypes in AD. (A) Clustering analysis based on the three UPGs (*USP3*, *HECW2* and *PSMB7*). (B,C) CDF curve and CDF delta area curve. (D) PCA diagram analysis of the three subclusters. (E,F) Boxplot and heatmap analysis of the three UPGs among subclusters. *** represents $p < 0.001$. CDF, cumulative distribution function; PCA, principal component analysis.

HECW2, and *PSMB7* are shown in the boxplot and heatmap (Fig. 6E,F). *USP3* had higher expression levels in cluster 2 than the other two clusters, while *HECW2* and *PSMB7* had higher expression levels in cluster 1 than the other two clusters (Fig. 6E,F).

3.5.4 GSVA of Pathways among Subclusters of UPGs

The GSVA analysis revealed several pathways with differential expression that were enriched. As shown in **Supplementary Fig. 2A**, TGF- β signaling, interferon- α response, inflammatory response, interferon- γ response, TNF- α signaling via NF- κ B, IL2-STAT5, and IL6-JAK-STAT3 signaling were higher in clusters 2 and 3, while DNA repair, glycolysis, and PI3K-AKT-mTOR signaling were lower. Furthermore, ssGSEA analysis demonstrated that the expression of most immune cells was low in cluster 1 and high in clusters 2 and 3. Macrophages and neutrophils were highly expressed in cluster 2, while eosinophils and mast cells were highly expressed in cluster 3 (**Supplementary Fig. 2B**).

3.5.5 Verification of the Diagnostic Efficacy of the Riskscore.

We further validated the diagnostic efficacy of the riskscores using GEO data sets. We found the area under the curve (AUC) of riskscores for GSE33000, GSE5281, GSE26972, GSE29378, GSE36980, and GSE63060 were 0.92, 0.8, 1.0, 0.734, 0.857, and 0.69, respectively. This was higher than that of age or gender (Fig. 7), suggesting the riskscore predictive model for AD was more advantageous than other clinical characteristics.

3.5.6 Validation of UPGs

RT-qPCR was used to detect the mRNA expression levels of the three UPGs in peripheral blood collected from the healthy controls and patients with AD. As shown in Fig. 8 and **Supplementary Fig. 3**, the expression level of *USP3* was significantly increased. *PSMB7* and *UBE2V1* were decreased in the AD group in comparison to controls, confirming the accuracy of our study.

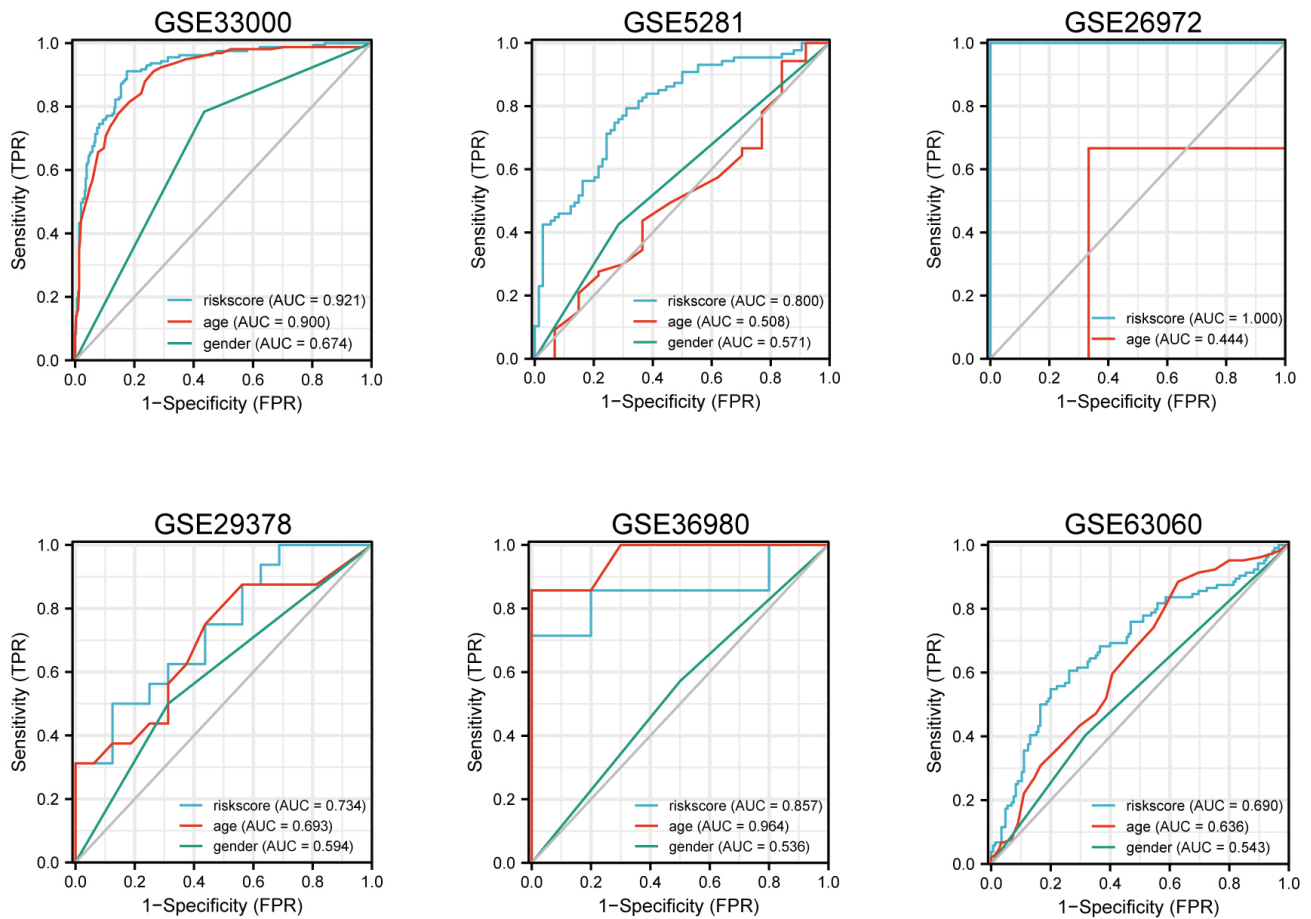


Fig. 7. Verification of the diagnostic efficacy of the risk score. ROC curve for the risk score. ROC, Receiver operating curve; TPR, true positive rate; FPR, false positive rate.

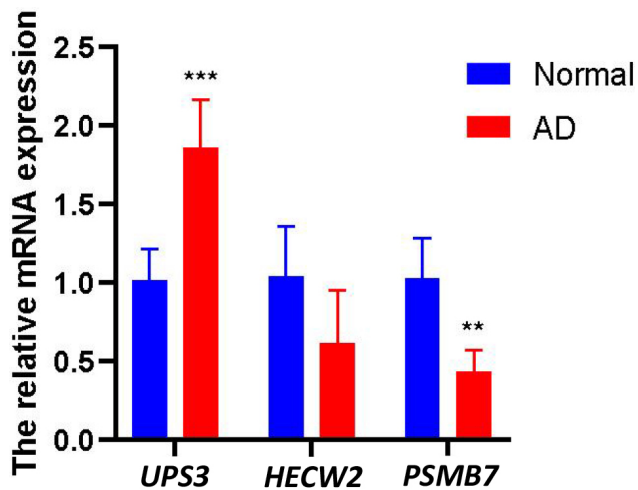


Fig. 8. Validation of the UPGs. The expression levels of three UPGs in the blood of healthy controls and AD patients were detected by RT-qPCR (real-time quantitative PCR) (n = 5). ** represents $p < 0.01$; *** represents $p < 0.001$.

4. Discussion

AD is the most common cause of dementia, with a high incidence and a heavy burden on society and families [32]. Unfortunately, there is no cure for AD. Thus, early prevention and diagnosis of AD is urgently needed. Some pathological features of AD have been identified, such as amyloid-beta ($A\beta$) peptide in cerebrospinal fluid [33], plasma p-Tau181 [34], and serum miR-24-3p [35]. Emerging studies report that the UPS is abnormally expressed in AD patients, resulting in dysregulation of protein degradation, which may promote AD progression. In this study, we screened the differentially expressed UPGs that were specifically associated with AD in GEO data sets and identified four UPGs (*USP3*, *HECW2*, *PSMB7*, and *UBE2V1*) by multiple bioinformatic analyses. Subsequently, three UPGs (*USP3*, *HECW2*, *PSMB7*), which are strongly correlated with the clinical features of AD, were used to construct a risk score prediction model to diagnose AD. Furthermore, we explored immune cell infiltration in the brain tissue of AD patients and the associations between immune cells and the three key UPGs. Finally, the risk score model was verified in several data sets of AD and showed good accuracy.

UPS dysfunction has been identified in the AD brain [18] and is associated with the A β production [17] and synaptic plasticity impairments seen in AD patients [19,20]. First, through KEGG analyses, we found that several pathways played important roles in the pathogenesis of AD. Recent studies have shown that HIF-1 signaling is a potential therapeutic target for AD [36]. HIF-1 signaling inhibits tau hyperphosphorylation and nerve filament formation [37]. Then, we identified three UPGs (*USP3*, *HECW2*, *PSMB7*), which are strongly correlated to the clinical features of AD. *USP3* is responsible for protein deubiquitination and metabolism. It has also been identified to deubiquitinate and stabilize Kruppel-Like Factor 5 (KLF5), promoting the proliferation of breast cancer cells [38,39]. KLF5 could bind to the Beta-Site APP Cleaving Enzyme 1 (BACE1) promoter to promote A β synthesis and accelerate the progression of AD [40]. Consistently, our study found that *USP3* is highly expressed in the brain of AD patients and is positively associated with amyloid-beta 42 levels. It is probable that *USP3* may induce AD by deubiquitinating KLF5 to promote A β production. Thus, targeting *USP3* may be a potential therapeutic strategy, which deserves further investigation.

HECW2, an E3 ubiquitin ligase and ubiquitin protein transferase, has an essential role in regulating neural crest cell development [41]. Studies have found that HECW2 positively regulates the proliferation of intestinal neuroprecursors by Glial Cell Derived Neurotrophic Factor (GDNF) [42]. GDNF could reduce the toxicity induced by amyloid beta [43], however the serum GDNF level in AD patients is significantly decreased [44]. Recently, a HECW2 mutation was reported to be related to neurodevelopmental disorders associated with hypotonia, seizures, and absent language [45]. In this study, we found that HECW2 was significantly decreased in the brain of AD patients and we speculate the reduction of HECW2 in brain may inhibit the expression of GDNF and aggravate the severity of AD. However, further investigation is needed.

PSMB7, a subunit of the proteasome, is reported to be involved in anthracycline resistance in breast cancer and bortezomib resistance in multiple myeloma [46,47]. Down-regulation of PSMA7 has been found to be involved in amyloid precursor protein-induced neural stem cell proliferation impairment, thereby promoting AD pathogenesis [48]. Consistently, our study found that PSMA7 was significantly decreased in the brain of AD patients and was negatively related to alpha secretase and gamma secretase activity. Overall, our study identifies three key UPGs (*USP3*, *HECW2*, *PSMB7*) that are strongly correlated to the clinical features of AD and established a riskscore prediction model based on these three UPGs, which shows good accuracy for predicting the severity of AD. The detailed roles of these three UPGs in AD development is worth further investigation.

Based on the three key UPGs, we performed unsupervised cluster analyses to identify three distinct clusters. A GSVA analysis showed DNA repair, glycolysis, and PI3K-AKT-mTOR signaling pathways were enriched in cluster 1 and TGF- β signaling, interferon- α response, inflammatory response, interferon- γ response, TNF- α signaling via NF- κ B, IL2-STAT5, and IL6-JAK-STAT3 signaling pathways were enriched in clusters 2 and 3. In addition, ss-GSEA analysis showed activated B cells, CD56dim natural killer cells, effector memory CD8 T cells, and Type 17 T helper cells had low expression in cluster 1. Macrophages and neutrophils [49,50] were highly expressed in cluster 2, and mast cells and eosinophils were highly expressed in cluster 3. By analyzing the relationship between the gene expression of the three clusters and clinical characteristics, cluster 1 was found to have the mildest clinical characteristics, while cluster 2 had the heaviest clinical characteristics. Previous studies found that AD patients' brain tissue had infiltrated macrophages, neutrophils, mast cells, and eosinophils [51,52]. The pathological changes and inflammatory mechanism of AD caused by the infiltration of these immune cells need to be further studied.

This study had some limitations. For example, the Ubiquitin-Proteasomal system-related hub genes as novel biomarkers for AD were screened using the GEO public database with relatively small sample sizes. More samples are needed in the future studies. Second, the hub genes expressed in the blood of AD patients' needs to be validated with more clinical samples. Third, the cor-relationship between the expressions of hub genes and the severity of AD should be analyzed with patients' clinical characteristics and imaging data. Further large-scale basic studies could be carried out to verify the conclusions of this study.

5. Conclusions

Our study identified 3 key UPGs that are specifically associated with AD and established a nomogram to predict the probability of AD. Furthermore, we explored the patterns of immune cells in the brain tissue of AD patients and the associations between immune cells and three key UPGs as potential biomarkers of AD. However, the specific roles of these key UPGs in AD still needs to be further investigated through molecular experiments.

Abbreviations

AD, Alzheimer's disease; UPS, Ubiquitin-Protease system; UPGs, UPS-related genes; A β , Amyloid-beta; GEO, Gene Expression Omnibus; DSM-IV, Diagnostic and Statistical Manual of Mental Disorders; DEGs, Differentially expressed genes; BP, Biologic processes; CC, Cellular components; MF, Molecular functions; ROC, Receiver operating curve; USP3, Ubiquitin specific peptidase 3; HECW2, C2, HECT, and WW domain containing E3 ubiquitin protein ligase 2; PSMB7, proteasome 20S subunit beta 7; UBE2V1, ubiquitin-conjugating enzyme E2 variant 1.

Availability of Data and Materials

The data analyzed in the present study are publicly available on the GEO database. The datasets used and/or analysed during the current study are available from the corresponding author on reasonable request.

Author Contributions

YZ, JZ and LZ designed, supervised the study, and supported funding acquisition. YZ, JW, GY, WG, YW, ZY, YG, and QZ performed the experiment. YZ, JW, GY, WG, YW, ZY, YG, and QZ analyzed the data. YZ, JW, GY, WG, YW, ZY, YG, and QZ wrote the manuscript. YZ, JW, GY, WG, YW, ZY, YG, and QZ constructed the figures and revised the manuscript. YZ, JZ and LZ finalized the paper. All authors contributed to editorial changes in the manuscript. All authors read and approved the final manuscript. All authors read and approved the final manuscript. All authors have participated sufficiently in the work and agreed to be accountable for all aspects of the work.

Ethics Approval and Consent to Participate

The study protocol was approved by the Ethics Committee of the Guangdong Second Provincial Hospital (20191121-01-YXKXYJ-SZRLH2020) and adhered to the tenets of the Declaration of Helsinki. Informed consent was obtained from the patients.

Acknowledgment

Not applicable.

Funding

This study was supported by the Science and Technology Planning Project of Guangzhou (202201010966), the Science and Technology Commissioner Project of Guangdong Province (GDKTP2021003800), The fifth batch of national TCM clinical outstanding talents training project (2021271) and the Scientific Research Project of Guangdong Provincial Bureau of Traditional Chinese Medicine (20231017).

Conflict of Interest

The authors declare no conflict of interest.

Supplementary Material

Supplementary material associated with this article can be found, in the online version, at <https://doi.org/10.31083/j.jim2206138>.

References

- [1] Puangmalai N, Sengupta U, Bhatt N, Gaikwad S, Montalbano M, Bhuyan A, *et al.* Lysine 63-linked ubiquitination of tau oligomers contributes to the pathogenesis of Alzheimer's disease. *The Journal of Biological Chemistry*. 2022; 298: 101766.
- [2] Roda AR, Serra-Mir G, Montoliu-Gaya L, Tiessler L, Villegas S. Amyloid-beta peptide and tau protein crosstalk in Alzheimer's disease. *Neural Regeneration Research*. 2022; 17: 1666–1674.
- [3] Feng L, Li J, Zhang R. Current research status of blood biomarkers in Alzheimer's disease: Diagnosis and prognosis. *Ageing Research Reviews*. 2021; 72: 101492.
- [4] Haoudy S, Jonveaux T, Puisieux S, Epstein J, Hopes L, Maillard L, *et al.* Epilepsy in Early Onset Alzheimer's Disease. *Journal of Alzheimer's Disease*. 2022; 85: 615–626.
- [5] Lee WJ, Brown JA, Kim HR, La Joie R, Cho H, Lyoo CH, *et al.* Regional A β -tau interactions promote onset and acceleration of Alzheimer's disease tau spreading. *Neuron*. 2022; 110: 1932–1943.e5.
- [6] Barbier M, Wallon D, Le Ber I. Monogenic inheritance in early-onset dementia: illustration in Alzheimer's disease and frontotemporal lobar dementia. *Geriatric et Psychologie Neuropsychiatrie Du Vieillessement*. 2018; 16: 289–297.
- [7] Moussa-Pacha NM, Abdin SM, Omar HA, Alniss H, Al-Tel TH. BACE1 inhibitors: Current status and future directions in treating Alzheimer's disease. *Medicinal Research Reviews*. 2020; 40: 339–384.
- [8] Tolar M, Hey J, Power A, Abushakra S. Neurotoxic Soluble Amyloid Oligomers Drive Alzheimer's Pathogenesis and Represent a Clinically Validated Target for Slowing Disease Progression. *International Journal of Molecular Sciences*. 2021; 22: 6355.
- [9] Roy PK, Biswas A, K D, Mandal M. An insight into the ubiquitin-proteasomal axis and related therapeutic approaches towards central nervous system malignancies. *Biochimica et Biophysica Acta. Reviews on Cancer*. 2022; 1877: 188734.
- [10] Baek D, Park KH, Lee KM, Jung S, Joung S, Kim J, *et al.* Ubiquitin-specific protease 53 promotes osteogenic differentiation of human bone marrow-derived mesenchymal stem cells. *Cell Death & Disease*. 2021; 12: 238.
- [11] Liu C, Yao X, Li M, Xi Y, Zhao L. USP39 regulates the cell cycle, survival, and growth of human leukemia cells. *Bioscience Reports*. 2019; 39: BSR20190040.
- [12] Wu J, Kumar S, Wang F, Wang H, Chen L, Arsenault P, *et al.* Chemical Approaches to Intervening in Ubiquitin Specific Protease 7 (USP7) Function for Oncology and Immune Oncology Therapies. *Journal of Medicinal Chemistry*. 2018; 61: 422–443.
- [13] Andres AM, Stotland A, Queliconi BB, Gottlieb RA. A time to reap, a time to sow: mitophagy and biogenesis in cardiac pathophysiology. *Journal of Molecular and Cellular Cardiology*. 2015; 78: 62–72.
- [14] Ren Z, Liu Z, Ma S, Yue J, Yang J, Wang R, *et al.* Expression and clinical significance of UBE2V1 in cervical cancer. *Biochemistry and Biophysics Reports*. 2021; 28: 101108.
- [15] Salminen A, Kaamiranta K, Kauppinen A, Ojala J, Haapasalo A, Soininen H, *et al.* Impaired autophagy and APP processing in Alzheimer's disease: The potential role of Beclin 1 interactome. *Progress in Neurobiology*. 2013; 106–107: 33–54.
- [16] Walden H, Muqit MMK. Ubiquitin and Parkinson's disease through the looking glass of genetics. *The Biochemical Journal*. 2017; 474: 1439–1451.
- [17] Gentier RJG, Verheijen BM, Zamboni M, Stroeken MMA, Hermes DJHP, Küsters B, *et al.* Localization of mutant ubiquitin in the brain of a transgenic mouse line with proteasomal inhibition and its validation at specific sites in Alzheimer's disease. *Frontiers in Neuroanatomy*. 2015; 9: 26.
- [18] Necchi D, Lomoio S, Scherini E. Dysfunction of the ubiquitin-proteasome system in the cerebellum of aging Ts65Dn mice. *Experimental Neurology*. 2011; 232: 114–118.
- [19] Hong L, Huang HC, Jiang ZF. Relationship between amyloid-beta and the ubiquitin-proteasome system in Alzheimer's disease. *Neurological Research*. 2014; 36: 276–282.

- [20] Vriend J, Ghavami S, Marzban H. The role of the ubiquitin proteasome system in cerebellar development and medulloblastoma. *Molecular Brain*. 2015; 8: 64.
- [21] Chen L, Wang C, Sun H, Wang J, Liang Y, Wang Y, *et al*. The bioinformatics toolbox for circRNA discovery and analysis. *Briefings in Bioinformatics*. 2021; 22: 1706–1728.
- [22] Gauthier J, Vincent AT, Charette SJ, Derome N. A brief history of bioinformatics. *Briefings in Bioinformatics*. 2019; 20: 1981–1996.
- [23] Wang J, Li J, Zhang L, Qin Y, Zhang F, Hu R, *et al*. Comprehensive analysis of ubiquitin-proteasome system genes related to prognosis and immunosuppression in head and neck squamous cell carcinoma. *Aging*. 2021; 13: 20277–20301.
- [24] Che Y, Jiang D, Xu L, Sun Y, Wu Y, Liu Y, *et al*. The Clinical Prediction Value of the Ubiquitination Model Reflecting the Immune Traits in LUAD. *Frontiers in Immunology*. 2022; 13: 846402.
- [25] Zenaro E, Pietronigro E, Della Bianca V, Piacentino G, Marongiu L, Budui S, *et al*. Neutrophils promote Alzheimer's disease-like pathology and cognitive decline via LFA-1 integrin. *Nature Medicine*. 2015; 21: 880–886.
- [26] Zhang Y, Fung ITH, Sankar P, Chen X, Robison LS, Ye L, *et al*. Depletion of NK Cells Improves Cognitive Function in the Alzheimer Disease Mouse Model. *Journal of Immunology*. 2020; 205: 502–510.
- [27] Ritchie ME, Phipson B, Wu D, Hu Y, Law CW, Shi W, *et al*. limma powers differential expression analyses for RNA-sequencing and microarray studies. *Nucleic Acids Research*. 2015; 43: e47.
- [28] Langfelder P, Horvath S. WGCNA: an R package for weighted correlation network analysis. *BMC Bioinformatics*. 2008; 9: 559.
- [29] Song L, Langfelder P, Horvath S. Comparison of co-expression measures: mutual information, correlation, and model based indices. *BMC Bioinformatics*. 2012; 13: 328.
- [30] Wei P, Dong M, Bi Y, Chen S, Huang W, Li T, *et al*. Identification and validation of a signature based on macrophage cell marker genes to predict recurrent miscarriage by integrated analysis of single-cell and bulk RNA-sequencing. *Frontiers in Immunology*. 2022; 13: 1053819.
- [31] Wilkerson MD, Hayes DN. ConsensusClusterPlus: a class discovery tool with confidence assessments and item tracking. *Bioinformatics*. 2010; 26: 1572–1573.
- [32] Chowdhury MR, Jin HK, Bae JS. Diverse Roles of Ceramide in the Progression and Pathogenesis of Alzheimer's Disease. *Biomedicines*. 2022; 10: 1956.
- [33] DeMattos RB, Bales KR, Cummins DJ, Dodart JC, Paul SM, Holtzman DM. Peripheral anti-A beta antibody alters CNS and plasma A beta clearance and decreases brain A beta burden in a mouse model of Alzheimer's disease. *Proceedings of the National Academy of Sciences of the United States of America*. 2001; 98: 8850–8855.
- [34] Suárez-Calvet M, Karikari TK, Ashton NJ, Lantero Rodríguez J, Milà-Alomà M, Gispert JD, *et al*. Novel tau biomarkers phosphorylated at T181, T217 or T231 rise in the initial stages of the preclinical Alzheimer's continuum when only subtle changes in A β pathology are detected. *EMBO Molecular Medicine*. 2020; 12: e12921.
- [35] Liu L, Liu L, Lu Y, Zhang T, Zhao W. Serum aberrant expression of miR-24-3p and its diagnostic value in Alzheimer's disease. *Biomarkers in Medicine*. 2021; 15: 1499–1507.
- [36] Wang YY, Huang ZT, Yuan MH, Jing F, Cai RL, Zou Q, *et al*. Role of Hypoxia Inducible Factor-1 α in Alzheimer's Disease. *Journal of Alzheimer's Disease*. 2021; 80: 949–961.
- [37] Merelli A, Rodríguez JCG, Folch J, Regueiro MR, Camins A, Lazarowski A. Understanding the Role of Hypoxia Inducible Factor During Neurodegeneration for New Therapeutics Opportunities. *Current Neuropharmacology*. 2018; 16: 1484–1498.
- [38] Zhuang W, Zhang L, Zheng Y, Liu B, Ma C, Zhao W, *et al*. USP3 deubiquitinates and stabilizes the adapter protein ASC to regulate inflammasome activation. *Cellular & Molecular Immunology*. 2022; 19: 1141–1152.
- [39] Wu Y, Qin J, Li F, Yang C, Li Z, Zhou Z, *et al*. USP3 promotes breast cancer cell proliferation by deubiquitinating KLF5. *The Journal of Biological Chemistry*. 2019; 294: 17837–17847.
- [40] Wang Y, Cui Y, Liu J, Song Q, Cao M, Hou Y, *et al*. Krüppel-like factor 5 accelerates the pathogenesis of Alzheimer's disease via BACE1-mediated APP processing. *Alzheimer's Research & Therapy*. 2022; 14: 103.
- [41] Berko ER, Cho MT, Eng C, Shao Y, Sweetser DA, Waxler J, *et al*. De novo missense variants in HECW2 are associated with neurodevelopmental delay and hypotonia. *Journal of Medical Genetics*. 2017; 54: 84–86.
- [42] Wei R, Qiu X, Wang S, Li Y, Wang Y, Lu K, *et al*. NEDL2 is an essential regulator of enteric neural development and GDNF/Ret signaling. *Cellular Signalling*. 2015; 27: 578–586.
- [43] Kitiyanant N, Kitiyanant Y, Svendsen CN, Thangnipon W. BDNF-, IGF-1- and GDNF-secreting human neural progenitor cells rescue amyloid β -induced toxicity in cultured rat septal neurons. *Neurochemical Research*. 2012; 37: 143–152.
- [44] Sharif M, Noroozian M, Hashemian F. Do serum GDNF levels correlate with severity of Alzheimer's disease? *Neurological Sciences*. 2021; 42: 2865–2872.
- [45] Yanagishita T, Hirade T, Shimojima Yamamoto K, Funatsuka M, Miyamoto Y, Maeda M, *et al*. HECW2-related disorder in four Japanese patients. *American Journal of Medical Genetics. Part a*. 2021; 185: 2895–2902.
- [46] Munkácsy G, Abdul-Ghani R, Mihály Z, Tegze B, Tchernitsa O, Surowiak P, *et al*. PSMB7 is associated with anthracycline resistance and is a prognostic biomarker in breast cancer. *British Journal of Cancer*. 2010; 102: 361–368.
- [47] Wu D, Miao J, Hu J, Li F, Gao D, Chen H, *et al*. PSMB7 Is a Key Gene Involved in the Development of Multiple Myeloma and Resistance to Bortezomib. *Frontiers in Oncology*. 2021; 11: 684232.
- [48] Wu Y, Zhang S, Xu Q, Zou H, Zhou W, Cai F, *et al*. Regulation of global gene expression and cell proliferation by APP. *Scientific Reports*. 2016; 6: 22460.
- [49] Mammana S, Fagone P, Cavalli E, Basile MS, Petralia MC, Nicoletti F, *et al*. The Role of Macrophages in Neuroinflammatory and Neurodegenerative Pathways of Alzheimer's Disease, Amyotrophic Lateral Sclerosis, and Multiple Sclerosis: Pathogenetic Cellular Effectors and Potential Therapeutic Targets. *International Journal of Molecular Sciences*. 2018; 19: 831.
- [50] Pietronigro EC, Della Bianca V, Zenaro E, Constantin G. NETosis in Alzheimer's Disease. *Frontiers in Immunology*. 2017; 8: 211.
- [51] Akdis CA. Does the epithelial barrier hypothesis explain the increase in allergy, autoimmunity and other chronic conditions? *Nature Reviews. Immunology*. 2021; 21: 739–751.
- [52] Shaik-Dasthagirisahab YB, Conti P. The Role of Mast Cells in Alzheimer's Disease. *Advances in Clinical and Experimental Medicine*. 2016; 25: 781–787.